Article

Modular total synthesis and cell-based anticancer activity evaluation of ouabagenin and other cardiotonic steroids with varying degrees of oxygenation.

Hem Raj Khatri, Bijay Bhattarai, Will Kaplan, Zhongzheng Li, Marcus John Curtis Long, Yimon Aye, and Pavel Nagorny

J. Am. Chem. Soc., **Just Accepted Manuscript** • DOI: 10.1021/jacs.8b12870 • Publication Date (Web): 25 Feb 2019

Modular total synthesis and cell-based anticancer activity evaluation of ouabagenin and other cardiotonic steroids with varying degrees of oxygenation.

Hem Raj Khatri,[†] Bijay Bhattarai,[†] Will Kaplan,[†] Zhongzheng Li,[$] Marcus John Curtis Long,*[#] Yimon Aye*[#¶] and Pavel Nagorny*[†]

[†]Chemistry Department, University of Michigan, Ann Arbor, MI 48109 USA

¶École Polytechnique Fédérale de Lausanne, Institute of Chemical Sciences and Engineering, 1015, Lausanne, Switzerland

#Department of Chemistry and Chemical Biology, Cornell University, Ithaca, NY 14853 USA

$Department of Chemistry, Nankai University, Nankai, People Republic of China

Cardiotonic steroids, Ouabagenin, Sarmentologenin, Total synthesis, Cascade reactions, Glycosylation, Anticancer activity

ABSTRACT: A Cu(II)-catalyzed diastereoselective Michael/aldol cascade approach is used to accomplish concise total syntheses of cardiotonic steroids with varying degrees of oxygenation including cardenolides ouabagenin, sarmentologenin, 19-hydroxysarmentogenin, and 5-*epi*-panogenin. These syntheses enabled the subsequent SAR studies on 37 synthetic and natural steroids to elucidate the effect of oxygenation, stereochemistry, C3-glycosylation and C17-heterocyclic ring. Based on this parallel evaluation of synthetic and natural steroids and their derivatives, glycosylated steroids cannogenol-*L*-α-rhamnoside (**79a**), strophanthidol-*L*-α-rhamnoside (**92**), and digitoxigenin-*L*-α-rhamnoside (**97**) were identified as the most potent steroids demonstrating broad anticancer activity at 10-100 nM concentrations and selectivity (nontoxic at 3 μM against NIH-3T3, MEF and developing fish embryos). Further analyses indicate that these molecules show a general mode of anticancer activity involving DNA damage upregulation that subsequently induces apoptosis.

1. INTRODUCTION

Cardiotonic steroids are a group of natural products that include cardenolides and bufadienolides.[1,2] Around a thousand different natural cardenolides and bufadienolides have been isolated to date from plants and animals. In addition to variations in the C17 heterocycle and C3 glycosylation, structural variations arise due to the presence of multiple oxygenation sites and changes in the skeletal and substituent stereochemical configurations (Figure 1).[2]

The majority of cardenolides and bufadienolides possess cardiotonic activity, which is attributed to their ability to inhibit Na^+/K^+ATPase pumps within cardiac myocytes.[1,3] Recent findings also indicate additional signaling functions, e.g., regulation of renal sodium transport and arterial pressure as well as cell growth, differentiation, apoptosis, fibrosis, modulation of immunity and carbohydrate metabolism, and the control of various central nervous functions and behaviors.[3] Cardiotonic steroids have also been investigated as potential therapeutic agents with anti-cancer,[4] anti-viral,[5] anti-bacterial,[6] immunoregulatory,[7] neural outgrowth differentiative,[8] anti-inflammatory[9] and anti-hypertensive[10] properties. Notably, overwhelming evidence indicates cardiotonic steroids as potential anti-cancer therapeutics.[4a,11]

However, as with most electrophilic compounds, the selectivity of cardiotonic steroids for transformed cells and also their general utility for cancer therapy is debated. This question has proven difficult to answer because various model systems/comparisons used to assess therapeutic value have been criticized.[12] The mode(s) of action of cardiotonic steroids also remain poorly-understood. Many studies agree that these molecules induce one of the most common cell death pathways, apoptosis[13a,b,c]; however, modes other than apoptosis have also been proposed, including: autosis, [13d] autophagy-related, caspase-independent cell death; and anoikis, [13e] a caspase-independent loss of adherence leading to cell death. Modes of action may also be cell-type specific. Reversible quiescence, rather than death, was reported in neuroblastomas treated with ouabain.[14] Despite all compounds sharing a similar core structure, different modes of action have been proposed for different cardiotonic steroids. Even for the most-commonly proposed mode of cardiac steroid-induced activity, apoptosis, numerous mechanisms have been put forward, e.g., inhibition of Na^+/K^+-ATPase (inactivation of which is linked to apoptosis, especially in cancer cells[13d]); inhibition of HIF1a[15] transcription (an effect that is independent of Na^+/K^+-ATPase); and DNA damage.

DNA damage is an appealing mode of action that is used by numerous anticancer drugs. However, there is considerable lack of certainty surrounding this behavior. Several studies describe that cardiac steroids are *adjuvants* to DNA-damage inducers, including radiation,[16] and small-molecule genotoxins.[16a] In mice, the synergy of cardiac steroids with the toxicity of DNA-damage inducers requires an active immune system, consistent with immunogenic cell death[17] (that cannot occur in typical cell culture). But it is difficult to see how such behavior links directly to cardiotonic steroid-specific toxicity. Interestingly, a few studies have reported DNA-damage upregula-

tion independent of additional DNA-damage stimulation.[14] One study reports DNA-damage-inducing effects in K562 cells (a BCR-ABL-positive leukemia line) treated with only digitoxin. However, these effects were transient,[18] indicating that DNA damage was not the principal cause of toxicity. Furthermore, several DNA-damage markers are upregulated during apoptosis,[19] rendering it difficult to assign cause and effect without careful controls. Moreover, few studies have compared outputs between sensitive and resistant lines, thus it is unknown which effects are on pathway. Thus, several outstanding questions remain: (1) Do cardiac steroids target a common pathway? (2) Do these compounds have selectivity for transformed versus non-transformed lines? (3) Is apoptosis the key pathway in cardiac steroid toxicity? (4) Is DNA damage involved in death and does this precede apoptosis or is it a consequence? (5) Are these processes on-target or off-target? Finally, assuming favorable answers to these questions are reached, it would be helpful to establish a mechanistic probe that displays all the selectivity characteristics of cardenolides for downstream studies.

Figure 1. Examples of variations in the oxidation state and stereochemistry in cardiotonic steroids

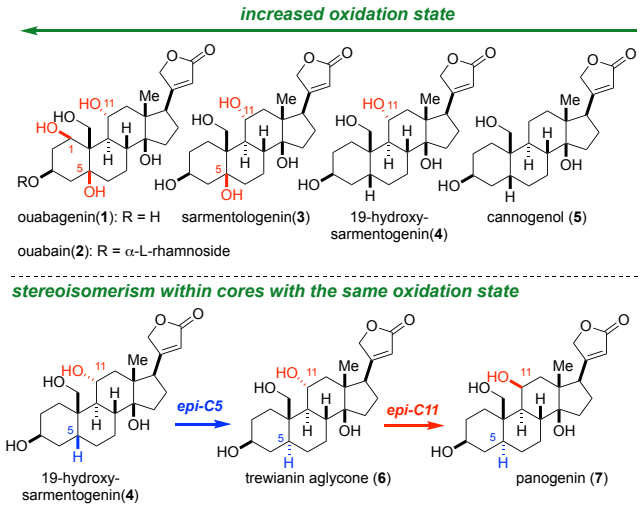

We propose that these key questions can be tackled by profiling toxicity/selectivity of a number of cardiotonic steroids across a panel of sensitive and insensitive cell lines. The SAR studies are scarce in terms of the structural features explored as they rely either on readily-available natural steroids or their semi-synthetic derivatives. Some aspects of SAR are known, e.g., C3 glycosylation is important for activity.[20] However, these conclusions do not always hold over numerous cell lines. A total synthesis-based route can potentially provide control over these parameters and thus enhance the medicinal exploration and optimization of cardiotonic steroids. However, the majority of the synthetic efforts towards the synthesis of cardiotonic steroids have focused on developing partial syntheses starting with androstane/pregnane derivatives.[21-23] Such routes are limited because readily-available androstanes and pregnanes often lack oxygenation at key positions of the steroid skeleton (i.e., at C1, C5, C11, C14, and C19). Some of these challenges were recently addressed by landmark studies on ouabagenin (**1**) and 19-hydroxysarmentogenin (**4**) by the Deslongchamps (Scheme 1a),[24] Baran (Scheme 1b)[25] and Inoue (Scheme 1c) laboratories.[26]

However, a general and flexible strategy to access cardiotonic steroids with various oxidation patterns is still highly desired. In our search for such a strategy, we focused on developing a convergent approach to steroidal cores **11** and **12** from relatively simple starting building blocks such as **8a** or **8b**. Rapid assembly of **11** and **12** and flexibility in adjusting the stereochemical configurations and oxidation state at the C5 and C11 positions in the subsequent manipulations are key in enabling the access to various cardenolides with varying degrees of oxygenation and with altered stereochemistry of the substituent- and ring-junction-bearing stereocenters (Scheme 1d).[27,28] These synthetic efforts are enabled by Cu(II)-catalyzed stereoselective Michael/aldol cascade reactions[27] allowing rapid assembly of functionalized steroidal skeletons **9** and **10**, which are then transposed to fully functionalized precursors **11** and **12** (6-7 steps, gram scale)[28] In this article, we apply this method to the concise total synthesis of highly-oxygenated cardenolides, ouabagenin (**1**) and sarmentologenin (**3**), and less oxidized steroids **4-7**, and numerous other analogs. With these compounds, we begin to address the critical biological questions above.

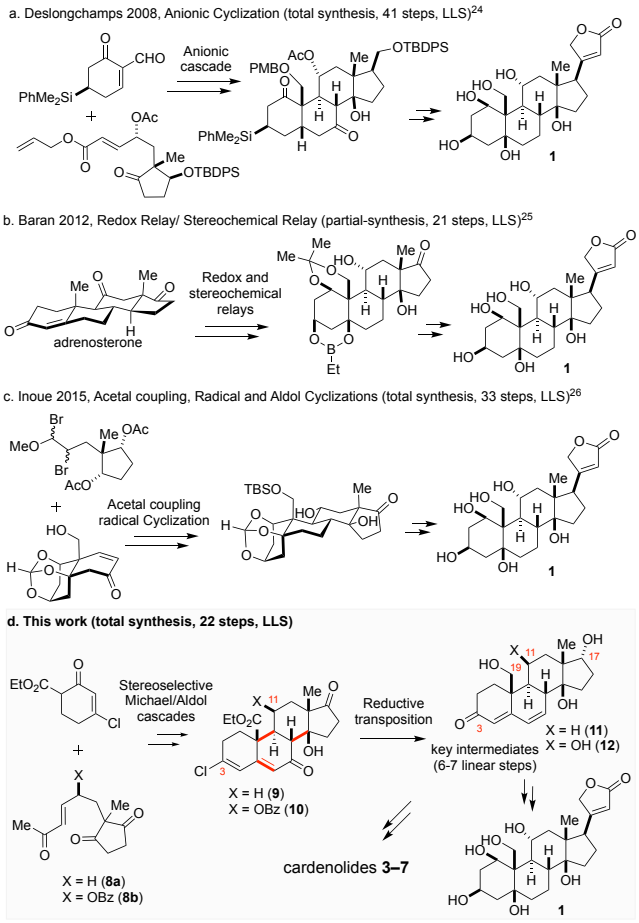

Scheme 1. Synthetic approaches to the highly oxygenated cardiotonic steroid, ouabagenin (1)

2. RESULTS AND DISCUSSION

We envisaged that a large subgroup of cardiotonic steroids containing C11 oxygenation could be accessed by a diastereoselective Cu(II)-catalyzed Michael reaction, providing rapid access to fully-functionalized steroidal intermediate with oxygenation at C3, 11, C14, C17 and C19 (Scheme 2A).[27] The

oxygenated intermediate thus accessed could then divergently be elaborated to various natural products following C14/C19 hydroxyl-controlled transformations.

We first undertook model studies to test the requisite diastereo-induction at C9 and C10 imposed by the C11 stereocenter (Scheme 2B).[28a,29] The $Cu(OTf)_2$-catalyzed Michael reaction of β–ketoester **13** and C11 oxygenated enone **14** proceeded with high levels of stereocontrol, yielding steroid **16** (44 % yield over 2-steps, >20:1 dr). As discussed previously,[27, 28a] the reaction likely proceeds via an open transition state **15** through a stepwise mechanism. An alternative mechanism involving a hetero-Diels–Alder reaction followed by the opening of the resultant ketal[29b] is less likely because ketoester **20** reacted equally well with *s*-trans dienes (cyclohexenone) under similar conditions (SI).

Our subsequent studies focused on developing the asymmetric variant of this reaction employing a chiral version of enone **14** and β–ketoester **19** containing the pre-installed C3 oxygenation (Scheme 2C). The enantioselective synthesis of enone **14** commenced with commercially-available 1,3-diketone **17** that was subjected to: Michael reaction with acrolein; organocatalytic oxidation[30] with benzoyl peroxide/catalyst **18**;[31] and Wittig reaction with commercially-available 1-(tripheylphosphoranylidene)-2-propanone to provide chiral enone **14** in 57% yield (3 steps) and 95% ee on a 20-g scale. Similarly, β-ketoester **20**, was obtained via acylation, acid-hydrolysis of ethyl-vinyl ether and chlorination.[28a] The key Michael reaction/double aldol cyclization cascade reaction proceeded smoothly and subsequent heating of the reaction mixture in acetonitrile with *p*-TSA at 70 °C for an additional 72 hours led to clean formation of compound **21** (45% yield, 1g scale).[28a]

Scheme 2. Diastereoselective Michael/aldol cascade reaction-based approach to ouabagenin (1) and related cardenolides

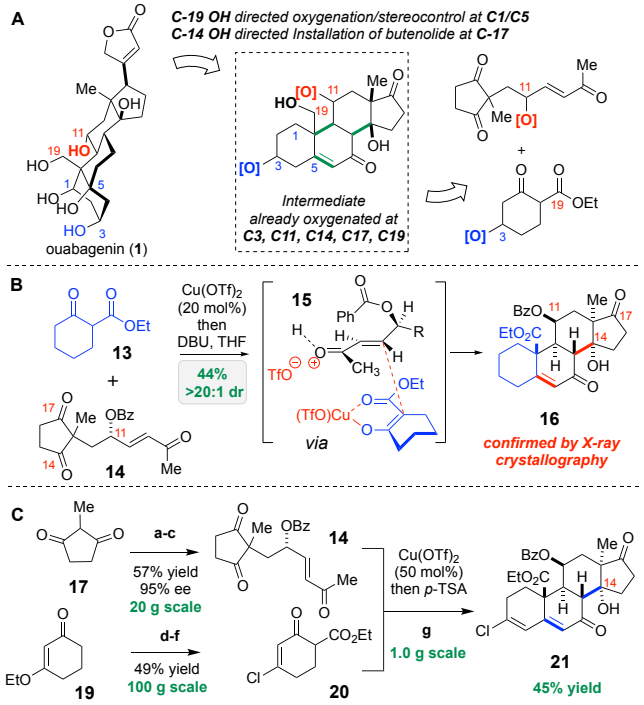

Reagents and conditions. **(Scheme 2B)**: **(a)** 20 mol% $Cu(OTf)_2$, rt, 12h, then 30 mol% DBU, THF, reflux, 12h. **(Scheme 2C)**: **(a)** acrolein, H_2O, 12 h, 97% yield; **(b)** 10 mol% (S)-2-(diphenyl((trimethylsilyl)oxy)methyl)pyrrolidine (**18**), $(BzO)_2$, hydroquinone, THF, H_2O, 1.5 h, 79% yield; **(c)** 1-(tripheylphosphoranylidene)-2-propanone, toluene, 75% yield; **(d)** LiHMDS, THF, -78 °C, 1h, then diethylcarbonate, rt, 12h, 73% yield; **(e)** 1 N HCl, THF: H_2O = 12:1, 6h, 84% yield; **(f)** PCl_3, $CHCl_3$, 0 °C to rt, 12h, 78% yield; **(g)** $Cu(OTf)_2$ (50 mol%), neat, rt, 12 h then add *p*-TSA (10 equiv), acetonitrile, 55 ºC, 72 h, 45% yield.

We pursued an approach relying on converting steroid **21** into key framework **12**, via intermediate **10** (Scheme **3**). Our calculations of the single point energy values of **21** and **10** (DFT, B3LYP, 6-31+G*, nonpolar solvent) indicated that diastereomer **10** is 2.0 kcal/mol more stable than **21**. Thus, we focused on isomerizing **21** into **10** under thermodynamic control.[26] Such isomerization could proceed under basic catalysis via retroaldolization of **21** to **22**, with intramolecular aldol of **22** giving **10**. Extensive optimization of the base, solvent and temperature showed that (Table 1-SI) Li^+ and K^+ counter-cations were not optimal (entries 1–3). However, Na^+-containing bases offered more promising results, with NaHMDS in toluene (entry 5, 6), giving **10** in 48% yield (68% brsm, 5.2 g scale) in >20:1 dr.

We next proposed that the global reduction of **10** would lead to pentaol **23**, which upon exposure to aqueous acid, would ionize to provide a delocalized carbocation. This carbocation would be trapped by water at C3, and the subsequent collapse of the unsaturated C3-chlorohemiacetal would form **12**.

Scheme 3. Epimerization and reductive transposition studies

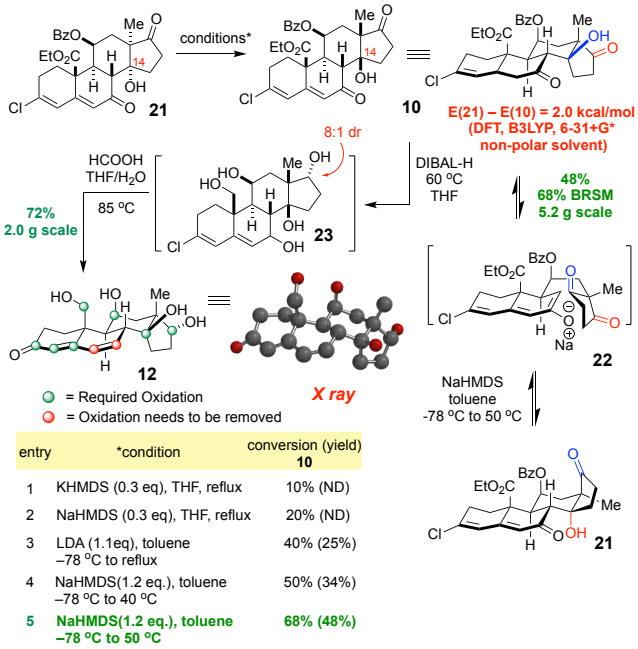

entry	*condition	conversion (yield) 10
1	KHMDS (0.3 eq), THF, reflux	10% (ND)
2	NaHMDS (0.3 eq), THF, reflux	20% (ND)
3	LDA (1.1eq), toluene –78 °C to reflux	40% (25%)
4	NaHMDS(1.2 eq.), toluene –78 °C to 40 °C	50% (34%)
5	**NaHMDS(1.2 eq.), toluene –78 °C to 50 °C**	**68% (48%)**

The global reduction of **10** turned out to be challenging. The use of $LiAlH_4$ yielded multiple products including those arising from dechlorination. $LiBH_4$ and DIBALH were slow to effect C19 ester reduction. However, DIBALH at 60 ºC in THF provided polyol **23**, which upon heating with aqueous formic acid in THF at 85 ºC provided **12** (2.0 g scale). The absolute and relative configuration of **12** was confirmed by X-ray crystallographic analysis.

Subsequent studies focused on converting **12** into 19-hydroxysarmentogenin (**4**) and related isomeric steroids [trewianin aglycone (**6**), panogenin (**7**), and 5-epi panogenin (**29**)] (Scheme 4). Approaches to **4**, **6**, **7** and **29** share the following features: (1) diastereoselective reduction of diene within **12** to form either β–C5 configuration present in **4** and **29** or α–C5 configuration present in **6** and **7**; (2) functionalization of the C11 position to invert its configuration (**4** and **6**) or to retain it (**7** and **29**); (3) installation of the C17 butenolide moiety based on the Stille coupling/hydrogenation sequence established by the Inoue and Baran groups.[25,26]

The direct hydrogenation of **12** with Pd/C as the catalyst could be directed by the unprotected C19 hydroxyl group to provide β–C5 stereocenter under basic conditions (Scheme 4A/4B). This event was followed by the selective C11/C19 acetonide protection leading to **24** (Scheme 4A) or by the C19 TIPS protection to provide intermediate **30** (Scheme 4B). The acetonide moiety in **24** was used to protect both the C19 as well as the β-C11 hydroxyls (Scheme 4A). As a result, the subsequent steps that included the oxidation of **24** with DMP (87% yield), and the elaboration of the oxidation product **25** to vinyl iodide **26** (79% yield, 2 steps) did not affect the stereochemistry of the C11 stereocenter. The subsequent Stille reaction with commercially available stannane **27** was carried out under the previously published conditions and provided precursor **28**. Similar to the observations of Inoue and Baran, we could not hydrogenate Δ^{16-17}–olefin in compound **28** directly to get a β–configured C17-butenolide. To circumvent this problem, **28** was reacted with TMSCl and imidazole in DMF forming the C14-protected product in 78% yield. The subsequent reduction proceeded with significantly higher selectivity than in the subsequent synthesis of **4** or **6**, providing a 25: 1.0: 2.8 mixture of α : β : Δ^{17-20}–olefin-containing product of deconjugation. This mixture was treated with HCl in methanol to provide 5-epi-panogenin (**29**) in 68% yield over 2 steps.

The elaboration of the intermediate **30** into 19-hydroxysarmentogenin (**4**) followed similar logic, but required additional steps required for the installation of the α-C11 stereocenter (Scheme 4B). This was carried out by subjecting **30** to oxidation with DMP and then performing subsequent site-selective reduction of the C3-ketone moiety with K-Selectride® (69% yield, >20:1 dr, 2 steps). The C17 ketone moiety of the resultant product **31** was selectively masked as a TBS-silyl enol ether (95% yield), and this product was subjected to the β-selective C11 ketone reduction with Li/NH_3 followed by the cleavage of the silyl enol ether moiety with TBAF (73% yield, 2 steps). The resultant product was then converted to vinyl iodide **32** with N_2H_4/ I_2 (90% yield), which was elaborated to 19-hydroxysarmentogenin (**4**) using the previously established strategy (4 steps, 25% yield).

Scheme 4. Synthesis of the isomeric cardenolides 19-hydroxysarmentogenin (4), trewianin aglycone (6), panogenin (7) and 5-epi panogenin (29)

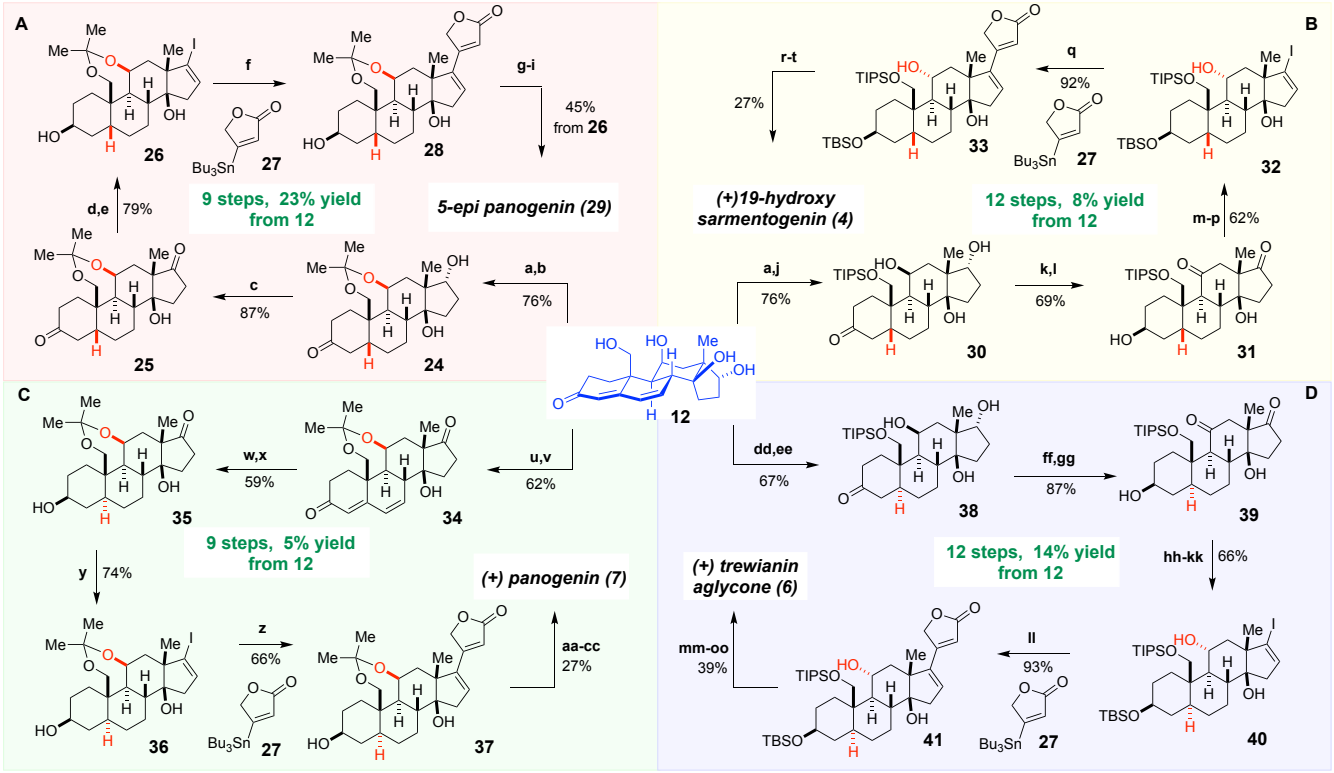

Reagents and conditions. **Scheme 4A (5-*epi* panogenin)**: **(a)** H_2, 10% Pd/C (25% w/w loading), KOH (1% w/v), quinoline (1% v/v), MeOH, 83% yield, >20:1 dr; **(b)** 2,2-dimethoxypropane, (+)-CSA, DMF, 91% yield; **(c)** DMP, CH_2Cl_2, 2 h, 87% yield; **(d)** K-Selectride®, THF, -78 to -30 °C, 45 min; >20:1 dr; **(e)** $N_2H_4 \cdot H_2O$, Et_3N, EtOH, 50 °C, 6 h then I_2, Et_3N, THF, rt, 1 h, 79% yield; **(f)** 4-(tributylstannyl)-2,5-dihydrofuran-2-one (**27**), $Pd(PPh_3)_4$, CuCl, LiCl, DMSO, 50 °C; **(g)** TMSCl, Imidazole, DMF, rt, 24 h, 66% yield, 2 steps; **(h)** H_2, Pd/C, EtOAc, 1 h; **(i)** 0.3 M HCl in MeOH, 1 h 68% yield, 2 steps; **Scheme 4B (19-hydroxysarmentogenin)**: **(j)** TIPSCl, ImH, DMF, rt, 6 h, 82% yield; **(k)** DMP, Py, CH_2Cl_2, 2 h, 89% yield; **(l)** K-Selectride®, THF, –78 to –30 °C, 1.5 h, 77% yield, >20:1 dr; **(m)** TBSOTf, Et_3N, CH_2Cl_2, –78 to –30 °C, 1.5 h, 95% yield; **(n)** Li, NH_3, THF, –78 °C, 30 min; **(o)** TBAF, THF, –78 °C, 5 min, 73% yield (2 steps); **(p)** $N_2H_4 \cdot H_2O$, Et_3N, EtOH, 50 °C, 6 h then I_2, Et_3N, THF, rt, 1 h, 90% yield; **(q)** 4-(tributylstannyl)-2,5-dihydrofuran-2-one (**27**), $Pd(PPh_3)_4$,

CuCl, LiCl, DMSO, 50 °C, 1 h, 92% yield; **(r)** TMSOTf, 2,6-lutidine, CH_2Cl_2, –78 °C to rt, 2 h, then SiO_2 (dry), 10 h, 64% yield; **(s)** H_2, Pd/C, EtOAc, 30 min, 2.7:1 dr (β-C17: α C17); **(t)** HF in $CH_3CN/H_2O/CH_2Cl_2$, rt, 3 days, 42% yield, 2 steps; **Scheme 4C (panogenin)**: **(u)** 2,2-dimethoxypropane, (+)-CSA, DMF, 69% yield; **(v)** DMP, Py, CH_2Cl_2, 1.5 h, 90% yield; **(w)** H_2, Pd/C (25% w/w), EtOAc/MeOH/CH_2Cl_2 (3:1:1), 20 min, 2.5:1 dr; **(x)** $LiAl(OtBu)_3H$, THF, –78 to –40 ºC; 2.5 h, 59% yield, >20:1 dr (2 steps); **(y)** $N_2H_4{\cdot}H_2O$, Et_3N, EtOH, 50 °C, 6 h then I_2, Et_3N, THF, rt, 1 h, 74% yield; **(z)** 4-(tributylstannyl)-2,5-dihydrofuran-2-one (**27**), $Pd(PPh_3)_4$, CuCl, LiCl, DMSO, 50 °C, 1 h, 66% yield; **(aa)** TMSOTf, 2,6-lutidine, CH_2Cl_2, –78 °C to rt, 2 h, then SiO_2 (dry), 10 h, 49% yield; **(bb)** H_2, Pd/C, EtOAc, 30 min; **(cc)** 0.3 M HCl in MeOH, 1 h 55% yield, 2 steps; **Scheme 4D (trewianin aglycone)**: **(dd)** TIPSCl, ImH, DMF, rt, 6 h, 81% yield; **(ee)** H_2, Pd/C, MeOH, Py, 4 h; 83% yield, >20:1 dr; **(ff)** DMP, Py, CH_2Cl_2, 2 h, 91% yield; **(gg)** $LiAlH(OtBu)_3$, THF, –78 to –40 °C, 4 h, 96% yield, >20:1 dr; **(hh)** TBSOTf, Et_3N, CH_2Cl_2, –78 to –30 °C, 1.5 h, 87% yield; **(ii)** Li, NH_3, THF, –78 °C, 30 min; **(jj)** TBAF, THF, –78 °C, 5 min, 91% yield (2 steps); **(kk)** $N_2H_4{\cdot}H_2O$, Et_3N, EtOH, 50 °C, 6 h then I_2, Et_3N, THF, rt, 1 h, 83% yield; **(ll)** 4-(tributylstannyl)-2,5-dihydrofuran-2-one (**27**), $Pd(PPh_3)_4$, CuCl, LiCl, DMSO, 50 °C, 1 h, 93% yield; **(mm)** TMSOTf, 2,6-lutidine, CH_2Cl_2, –78 °C to rt, 2 h, then SiO_2 (dry), 10 h, 79% yield; **(nn)** H_2, Pd/C, EtOAc, 30 min; 54% yield of β-C17 and 22% of α-C17; **(oo)** HF in $CH_3CN/H_2O/CH_2Cl_2$, 3 days, 91% yield.

The synthesis of the *trans*-A/B ring junction containing steroids panogenin (**7**) and trewianin aglycone (**6**) from 12 involved similar steps; however, required installation of the α-C5 stereocenter (Schemes 4C and 4D). The *trans*-A/B ring configuration of panogenin (**7**) was established by protecting the C11/C19 diol moiety of **12** as an acetonide, and oxidizing the C17 position with DMP to obtain intermediate **34** (62% yield, 2 steps) (Scheme 4C). This intermediate was hydrogenated over Pd/C to provide the product containing the *trans*-A/B ring junction (2.5:1 dr at C5), which was then reduced with $LiAlH(Ot\text{-}Bu)_3$ providing **35** (59% yield, 2 steps). This product was converted to vinyl iodide **36** (74% yield), which was subjected to 4 step butenolide installation sequence based on previously established for 5-epi-panogenin (**29**) route to provide **7** in 18% yield.

Finally, the synthesis of trewianin aglycone (**6**) commenced with the protection of the C19 group of **12** with as a TIPS ether (Scheme 4D). This bulky protecting group was essential for the highly selective hydrogenation with Pd/C to provide intermediate **38** with *trans*-A/B ring junction (>20:1 dr). The subsequent elaboration of **38** into **6** resembled the sequence developed for 19-hydroxysarmentogenin (**4**) and proceeded in 10 steps and 21% overall yield.

Scheme 5. Application to the synthesis of sarmentologenin (3)

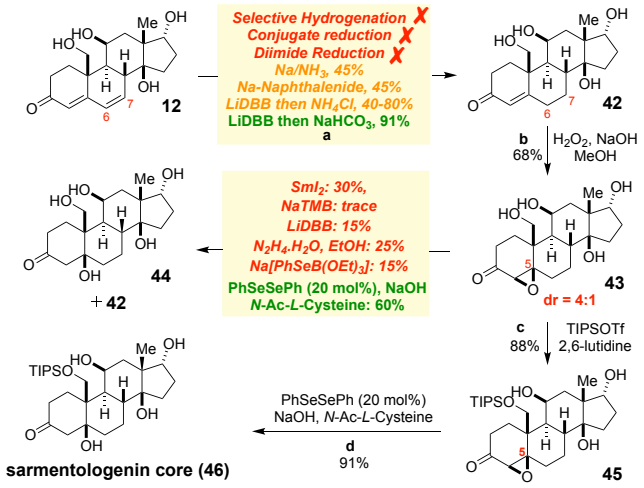

Reagents and conditions: **(a)** LiDBB, THF, -78 ºC, 15 min, then $NaHCO_3$, rt, 30 min, 91%; **(b)** H_2O_2, NaOH, MeOH, 0 ºC to rt, 2 h, 68%; **(c)** TIPSOTf, 2,6-lutidine, THF:CH_2Cl_2 = 1:1, 5 min, 88%; **(d)** PhSeSePh (20 mol%), *N*-Ac-*L*-Cysteine, NaOH, DMF, rt, 15 min, 91%.

The synthesis of sarementologenin (**3**) and ouabagenin (**1**) required developing an "oxidase phase" strategy for the selective reduction of the Δ^{6-7}–olefin of **12** and strategies for the installation of the oxygenation at the C1 and C5 positions.[32] The reduction of the Δ^6–olefin of **12** required extensive optimization (Scheme 5 and Table 4-SI) that identified LiDBB reduction followed by $NaHCO_3$ work up as the only viable option leading to **42**. The enone within **42** was epoxidized stereoselectively under basic conditions (68% yield, 4:1 dr) with β–epoxide **43** as the major product. Reduction of **43** presented another challenge because the reaction product, **44**, readily eliminated water, re-forming enone **42**. Numerous reported conditions for the selective reduction of **43** led to decomposition. The reduction promoted by PhSeSePh (10 mol%) and *N*-Ac-*L*-Cys-OH under basic conditions[33] was uniquely effective at accessing **44**.

Isolation of **44** was challenging due to its hydrophilicity. This issue was circumvented by selective TIPS protection of the C19-OH of **43** to provide **45** (88% yield). Epoxide **45** underwent facile ring opening under the optimized conditions for the epoxide opening [PhSeSePh (20 mol%), *N*-Ac-*L*-Cys, NaOH] to provide sarmentologenin core **46** in 91% yield.

Scheme 6. Completion of the synthesis of sarementologenin (3)

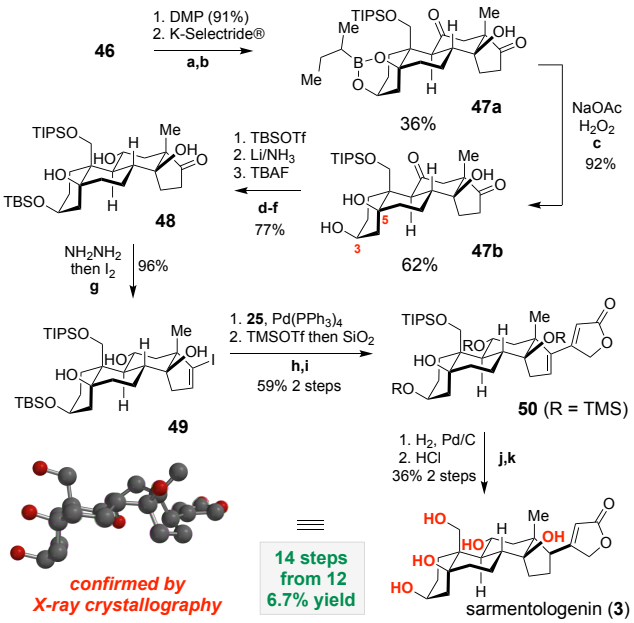

Reagents and conditions: **(a)** DMP, Py, CH_2Cl_2, rt, 2 h, 91% yield; **(b)** K-Selectride®, THF, -78 °C, 45 min, 62% yield for **47b**, 36% yield for **47a**; **(c)** H_2O_2, NaOAc, THF : H_2O = 3:1, rt, 16 h,

92% yield; **(d)** TBSOTf, Et_3N, CH_2Cl_2, -78 to -20 °C, 1 h, 88% yield; **(e)** Li, NH_3, THF, -78 °C, 15 min; **(f)** TBAF, THF, -78 °C, 5 min, 87% yield (2 steps); **(g)** $N_2H_4{\cdot}H_2O$, Et_3N, EtOH, 50 °C, 6 h then I_2, Et_3N, THF, rt, 1 h, 96% yield; **(h)** 4-(tributylstannyl)-2,5-dihydrofuran-2-one (**27**), $Pd(PPh_3)_4$, CuCl, LiCl, DMSO, 50 °C, 1 h; **(i)** TMSOTf, 2,6-lutidine, CH_2Cl_2, -78 °C to rt, 2 h, then SiO_2 (dry), 10 h, 52% yield (2 steps); **(j)** H_2, Pd/C, EtOAc, 30 min; 44% yield of β-C17 and 24% of α-C17; **(k)** HCl in MeOH, MeOH, rt, 30 min, 83% yield.

The sarmentologenin core **46** was then elaborated to sarementologenin (**3**) in 10 steps (Scheme 6). As before, the reduction of the C3 ketone moiety of **46** was accomplished with K-Selectride®. A stable boronic acid ester **47a** (36% yield) was obtained along with **47b** (62% yield); **47a** was hydrolyzed to **47b** with hydrogen peroxide/sodium acetate (92% yield). The key precursor **47b** was then subjected to the standard sequence (Scheme 6) that involved selective reduction from the α–face of the C11 ketone to provide **48** (77% yield, 3 steps), formation of the vinyl iodide **49** from **48** (89% yield) and stereoselective installation of the β–C17 butenolide moiety followed by an acid-mediated global deprotection to provide saremetologenin **3** (21% yield, 4 steps). The absolute and relative configuration of **3** was confirmed by X-ray crystallographic analysis.

Scheme 7. Initial studies towards the synthesis of ouabagenin (1)

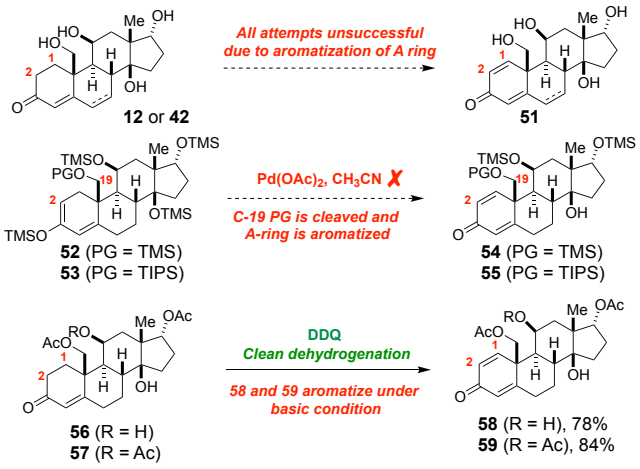

Our studies next focused on adapting the route to sarmentologenin (**3**) to the synthesis of ouabagenin (**1**). This required installation of an additional hydroxyl group at C1. We anticipated simultaneous installation of both hydroxyl groups from dienone **51** (Scheme 7) via epoxidation of both alkene positions and subsequent opening the resultant oxirane moieties using conditions developed in the synthesis of sarmentologenin (**3**). However, our attempts to obtain **51** or its protected variants, compounds **54** and **55**, were not successful due to facile aromatization of the steroidal A ring. The stability and reactivity of **54** and **55** could be improved by acetylation of the C19 hydroxyl group,[34] and the oxidation of **56** and **57** with DDQ provided dienones **58** and **59**, respectively. However, all attempts to accomplish selective epoxidation of **58** or **59** failed, so a stepwise installation of the C5 and C1 oxygenation through monoepoxide intermediate **43** was targeted next (Scheme 8).

Our studies commenced with the direct installation of the Δ^1–olefin in epoxide **43** using DDQ or selenium(IV) oxide, which led to enone **60** in low yields (30-50% yield) accompanied with unidentified and inseparable impurities (Scheme 8). An alternative route based on the dehydrogenation of *bis*-acetate **62** leading to **63** was investigated. The presence of the C19 acetate accelerated this oxidation relative to **43**, and the transformation of **62** to **63** was accomplished with selenium(IV) oxide or palladium(II) trifluoroacetate;[35] however, the yields for this transformation were low (~10-50%) and irreproducible due to concomitant cleavage and migration of acetates. The subsequent epoxidation of **63** to **61** was accomplished in 35% yield. Owing to the low efficiency and irreproducibility of several steps, this route was discarded. In search of a more efficient route, substrate **42** was acetylated (Ac_2O, DMAP) to provide triacetate **64** (89% yield), which was then selectively reduced from the α-face with K-Selectride® and subjected to C3-directed epoxidation with *m*-CPBA to provide epoxide **65** in 70% yield (6:1 dr for the epoxidation step) over 2 steps. The C3 alcohol moiety was oxidized with DMP to provide the corresponding C3 ketone, which was then subjected to various dehydrogenation conditions to establish the Δ^1–unsaturation. Unfortunately, oxidation with DDQ or SeO_2 did not efficiently form product **62** due to either epoxide opening or overoxidation at the C2 position leading to side-products (*vide supra*). However, directly oxidizing **65** with $Pd(TFA)_2$ under an atmosphere of oxygen furnished enone **66** in 89% yield.

Scheme 8. Installation of oxygenation in ouabagenin (1)

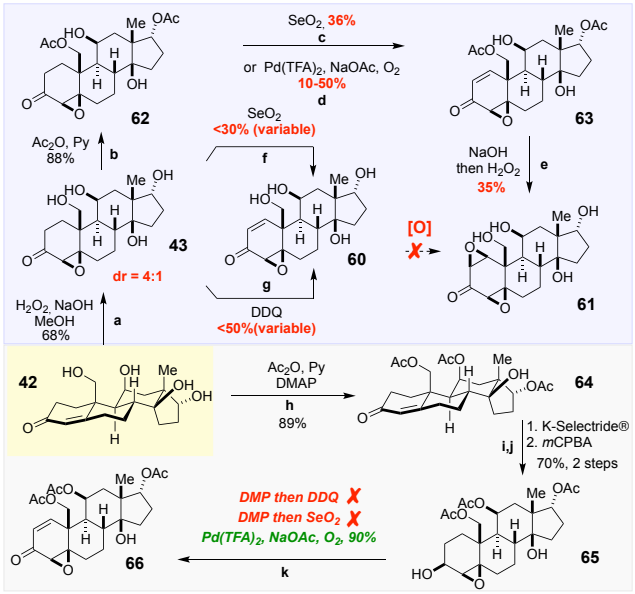

Reagents and conditions: **(a)** H_2O_2, NaOH, 0ºC to rt, 2 h, 68% yield; **(b)** Ac_2O, Py,rt, 2 h, 88% yield; **(c)** SeO_2, chlorobenzene, 90 ºC, 12 h, 36% yield (variable); **(d)** DDQ, dioxane, 90 ºC, 12 h, 10-50% yield(variable); **(e)** NaOH,MeOH, rt, 3 h, then H_2O_2, 0 ºC, 30 min, 35% yield; **(f)** SeO_2, chlorobenzene, 90 ºC, 12h, <30% yield (variable); **(g)** DDQ, dioxane, 90 ºC, 12 h, <50% yield (variable); **(h)** Ac_2O, Py, DMAP, rt, 16 h, 89% yield; **(i)** K-Selectride®, THF, -30 °C, 30 min, dr = 6:1; **(j)** *m*-CPBA, CH_2Cl_2, rt, 2 h, 70 % yield (2 steps); **(k)** $Pd(TFA)_2$, NaOAc, O_2, DMSO, 50 ºC, 36 h, 90% yield.

The installation of C1/C5 oxygenation *en route* to ouabagenin (**1**) was pursued next (Scheme 9). Subjecting **66** to LiOH then hydrogen peroxide resulted in the removal of the acetate protecting groups and installation of the C1/C2

Scheme 9. Completion of the synthesis of ouabagenin (1)

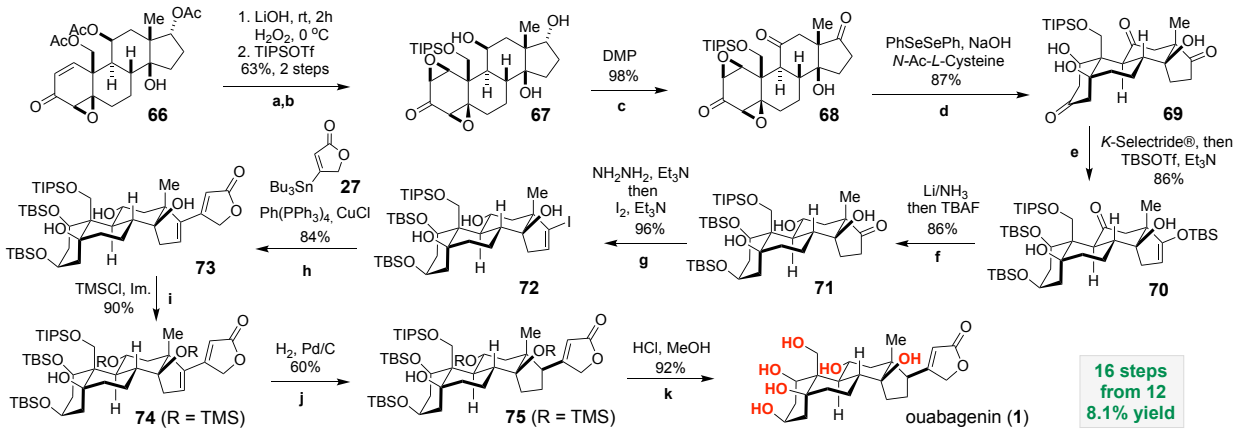

Reagents and conditions: **(a)** LiOH, MeOH, rt, 2 h, then H_2O_2, 0 ºC, 15 min, 74% yield; **(b)** TIPSOTf, 2,6-lutidine, THF, 5 min, 84% yield; **(c)** DMP, CH_2Cl_2, rt, 2 h, 98%; **(d)** PhSeSePh (20 mol%), *N*-Ac-*L*-Cysteine, NaOH, DMF, rt, 15 min, 87%; **(e)** K-Selectride®, THF, -78 °C, 30 min then TBSOTf, Et_3N, CH_2Cl_2, -20 °C, 30 min, 86% yield; **(f)** Li, NH_3, *t*-BuOH (10 equiv), THF, -78 °C, 15 min; then TBAF, THF, -20 °C, 8 h, 86% yield; **(g)** $N_2H_4 \cdot H_2O$, Et_3N, EtOH, 50 °C, 6 h then I_2, Et_3N, THF, rt, 1 h, 96% yield; **(h)** 4-(tributylstannyl)-2,5-dihydrofuran-2-one (**25**), $Pd(PPh_3)_4$, CuCl, LiCl, DMSO, 50 °C, 1 h, 84% yield; **(i)** TMSCl, Imidazole, DMF, rt, 72 h, 90% yield; **(j)** H_2, Pd/C, EtOAc, 30 min; 60%; **(k)** HCl in MeOH, MeOH, rt, 30 min, 92% yield.

epoxide (74% yield, single diastereomer). The C19 hydroxyl of the resultant *bis*-epoxide **61** was selectively protected as a TIPS ether giving compound **67** in 84% yield. This protection was important as it increased the hydrophobicity of **67**, a feature that was essential for the subsequent steps. The *bis*-epoxide moiety of **67** was oxidized with Dess-Martin reagent to provide triketone **68** in 98% yield, which was then subjected to the optimized conditions for the epoxide opening (PhSeSePh (20 mol%.), *N*-Ac-*L*-Cys, NaOH) that were developed during the studies on sarmentologenin (Scheme 6). Similar to previous reports from the Baran group,[21] we observed instability of **69** to water elimination and A-ring aromatization under basic or acidic conditions. Careful control of the *N*-Ac-*L*-Cys to NaOH stoichiometry was required to avoid these side reactions and obtain the desired product **69** in 87% yield. The C3 ketone moiety of **69** was then transformed to the C3- and C17-silylated enol ether **70** in 86% yield. Further elaboration of **70** proceeded through the standard sequence established for the other steroids and ultimately provided **75** (60% yield), which upon deprotection with HCl/MeOH yielded ouabagenin (**1**) in 92% yield. Our synthetic ouabagenin (**1**) was in all respects identical to the sample obtained by deglycosylation of ouabain (**2**), and its NMR spectra match previously published spectroscopic data.[24,25,26b,36] It should be noted that our total synthesis features only 22 linear steps and 1.0% overall yield.

We also targeted steroids lacking C11 oxygenation[37] (Scheme 10). This strategy was based on enantioselective Michael reaction of enone **8a** and β–ketoester **19a**, and it routinely led to the formation of the Michael adduct **76** in good yield, diastereoselectivity and enantioselectivity (92%, >20:1 dr, 92% ee) on 7.2 g scale. **76** was then elaborated to enone **11** via the sequence previously developed for its C11-hydroxy congener **12**. Substantial quantities of **11** were obtained and converted to cannogenol (**5**) in 9 steps and 20% overall yield. Since cannogenol 3-*O*-α–*L*-rhamnoside (**79a**), is a natural derivative of cannogenol (**5**) with anticancer activity in the nM range,[37] the synthesis of **79a** as well as other cannogenol glycosides **79b** and **79c** was pursued.[28b] To mask the more reactive C19 hydroxyl group, **5** was subjected to selective protection as a methoxyacetate to provide **77** (99% yield). The C3 alcohol of **77** was then glycosylated with trichloroacetimidate **78a** to provide the corresponding α-*L*-rhamnoside as the only diastereomer. The following deprotection of the sugar benzoates and C19 methoxyacetate leading to cannogenol α–*L*-rhamnoside (**79a**) required careful optimization due to the lability of the C17 butenolide under basic conditions. 50% ammonia in methanol achieved efficient cleavage of the ester moieties without destroying the butenolide (56% yield). This protocol was also employed to generate glycosides **79b** and **79c** in 22% and 65% yield from protected cannogenol derivative **77**. In addition to cannogenol (**5**) glycosides, the α–*L*-rhamnosides of steroids digitoxigenin,[20] bufalin[38] and strophanthidol[37] were synthesized using similar protocols (SI).

Poised to address the biological questions, we assayed a collection of 37 compounds (Table 11-SI) comprising those generated above and several commercially-available cardenolides (ouabain (**1**), *anhydro*-ouabagenin, digoxin, digitoxin, digitoxigenin, and strophanthidol). Our studies commenced with a smaller subgroup of synthetic aglycones **5, 6, 12, 100-105** (Table 11-SI) using different cell lines: HEK293T (an adenovirus-transformed cell line, containing the SV40 T-antigen); HeLa (a human cervical cancer line containing human papilloma virus 18); Cos7 (an African green monkey line expressing the SV40 T-antigen); Raji (a human Burkitt's lymphoma line); and NIH-3T3 (a mouse fibroblast line)]. This panel represents both adherent lines and a non-adherent line (Raji), and transformed lines, as well as a non-transformed line (NIH-3T3). Proliferation was measured over 2 days via AlamarBlue®. The assay was validated by comparing the normalized AlamarBlue signal averages of the DMSO-treated samples to those for cells treated with 2 μg/ml puromycin. A global z′ factor of 0.66 was observed between these two conditions. Compounds **5**, **6**, **12**, **100-105** were then screened at 2 μM and 0.6 μM. Only cannogenol (**5**) was active, showing activity against every line except NIH-3T3 at 2 μM, and affecting most lines at 0.6 μM. These data recapitulate previous findings that primate cell lines are sensitive to cardiotonic steroids, but rodent lines are unusually robust.[39] Furthermore, non-adherent lines were as sensitive as adherent lines, meaning anoikis is likely not an on-target death mechanism.

Scheme 10. Synthesis of cannogenol glycosides 79a-c

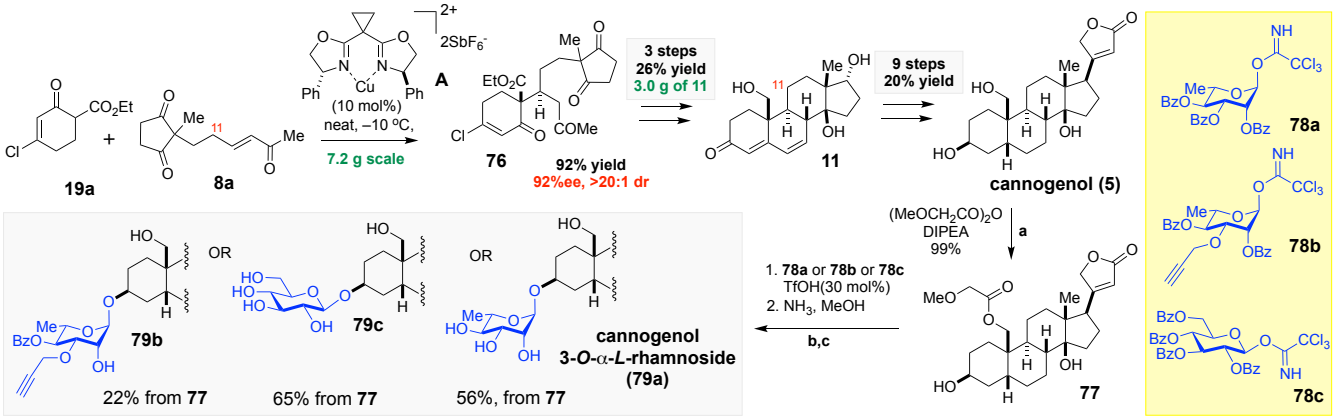

Reagents and conditions: **(a)** $(MeOCH_2CO)_2O$, DIPEA, CH_2Cl_2, 0 ºC, 12 h; **(b) 78a-c**, TfOH (30 mol%), CH_2Cl_2, 0 ºC, 5 h; **(c)** NH_3 (50% in MeOH), rt, 24 h, 56% from **77** for **79a**; 22% from **77** for **79b**; 65% from **77** for **79c**.

The EC_{50} of **5** in HEK293T was ~1 µM, consistent with the screening data.

We next took HEK293T (Figure 3A) and HeLa (Figure 3B) cells as representative sensitive lines and NIH-3T3 (Figure 2c-SI) as an insensitive line and assayed the 37 compounds for growth inhibition at 1 and 3 µM concentrations.

Figure 2. Summary of the key features from the SAR studies

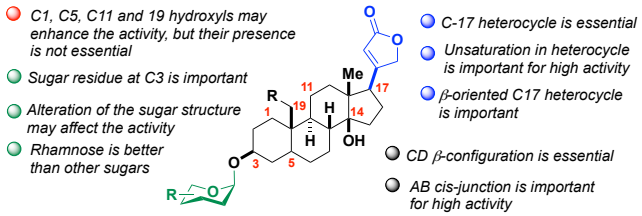

These studies enabled us to extract some important structure activity relationships (SAR). The significant SAR information is depicted in Figure 2 and are discussed in detail in supporting information (SI-2k). From these data, we also hoped to identify compounds highly toxic to HeLa and HEK293T but that did not affect NIH-3T3. If these characteristics were observed, we would preliminarily conclude that the compounds are on target. We evaluated EC_{50} values for the most potent compounds (none of which were toxic to NIH-3T3), most of them emerged to be glycosylated steroids (ouabagenin (**1**), ouabain (**2**), cannogenol α–*L*-rhamnoside (**79a**), **79c**, digitoxigenin (**80**), digitoxin (**81**), digoxin (**82**), and **92–98**), in HEK293T cells. These compounds showed EC_{50}s below 1 µM, consistent with the screens in Figures 3A and 3B.

The 5 most potent compounds (EC_{50}s below 100 nM in HEK293T cells) **81**, **82**, **79a**, **97** and **92** (Figure S3) were assayed against HeLa and several other cell lines (HepG2, a human hepatocellular carcinoma line; MDA-MB-231, a human invasive triple negative breast adenocarcinoma line; and U87, a human primary glioblastoma cell line), the results of which are depicted in Figure 3C. In HEK293T, **79a** was marginally more potent than **97** and **92**, and those 3 compounds were all approximately 2-3 fold more potent than **81** and digoxin **82**. This trend was retained in HeLa cells, but **79a** was marginally less toxic than **92** and **97**. In U87, HEPG2 and MDA-MB-231 **92** and **97** were significantly (up to 3-4 fold) more potent than **79a**. Furthermore, in HEPG2 the difference between **81** and **79a** was marginal although in the other lines **79a** was around 2-fold more potent than **81**. Considering that all these compounds were non-toxic to NIH-3T3 cells at 3 µM, *these data indicate that the toxicities were occurring via a conserved mechanism*.

Compound **79a** was next screened against several other lines [Cos7, Raji, HFF1 (a human fibroblast line), RAW (a virally-transformed mouse macrophage line), MEFs (a mouse embryonic fibroblast line) and HF-II-E (a hepatoma line from rat)] (Figure S4). The data observed were bimodal: either cells were sensitive to the compound at low-to-mid nanomolar concentrations or they were resistant to treatment (EC_{50}>1 µM). Similar outcomes were observed for other compounds (e.g. **98**, **97**, **79b**, and **99** were ineffective against RAW; **92**, and **97** were ineffective against HF-II-E; **98**, **81**, **2** and **1** were effective against HFF1 (Figure S4)) against the same lines. Thus, the toxicity was similar for numerous adherent cells versus the single non-adherent line, further arguing against anoikis as a prevalent mode of toxicity. Furthermore, the most active compounds were essentially non-toxic to non-cancerous lines, (NIH-3T3 and MEFS), but killed a wide range of different cancer cells, from humans and other species. *This observation could be considered as evidence that these compounds are selectively toxic to transformed cells.* However, these compounds were also non-toxic to transformed rodent lines and they were further unable to prevent human-RAS^{G12V} transformation of NIH-3T3 cells (Figure S5). Thus, although NIH-3T3 and other rodent cells are good model resistant lines, we provide very clear evidence— which is also consistent with previous reports[38,40]—that rodent lines are *generically* resistant to cardiac steroids. We assayed the effects of cardiac steroids on developing zebrafish relative to other cytotoxic compounds (Figure 2D). Zebrafish were chosen because numerous fish, including zebrafish, have been shown to be responsive to the cardiac steroid ouabain, and based on previous data and our own phylogenetic analysis, we expected Na,K-ATPase from zebrafish to be sensitive to cardiotonic steroids (Figure S6). Furthermore, hits from small-molecule screening in zebrafish have begun to enter clinical trials.[41]

We performed two assays, a teratogenicity assay, and assessment of the cardiac rate. Both assays involved dosing em-

bryos at the 2-8 cell stage. 3 μM **79a** [EC_{50}(HEK293T) = 0.015 μM] exhibited little toxicity or teratogenicity, although there was a slight increase in spinal curvature (Figure S7A). Mitomycin C [EC_{50}(HEK293T)=4 μM], brefeldin A [EC_{50}(HEK293T)=0.2 μM] and actinomycin D [EC_{50}(HEK293T)=0.002 μM] administered at 3 μM, all elicited significant toxicity and teratogenicity, although most of these compounds were less toxic to cancer cells than **79a** (Figure S7B). Heart rate was also unaffected by **79a** (Figure S7C). These results indicate that non-transformed cells tolerate **79a** much better than generically toxic compounds. This result underscores previous hypotheses concerning the suitability of these compounds as selective anticancer agents[13a] and is strongly consistent with the common use of these compounds in humans. Although more complex assays are required to define utility for anticancer treatment, these data are encouraging.

Interestingly, we found that cultured MDA-MB-231 cells treated with alkyne-functionalized **79b** (500 nM) followed by permeabilization, fixation, Click coupling to Cy5-azide, and extensive washing, exhibited intracellular fluorescence. DMSO-treated cells were less fluorescent. Since these assay conditions should only preserve irreversible adducts,[42] these data imply the presence of (an) intracellular protein(s) target(s) to which these compounds covalently bind (Figure S8). We are mindful that the principal biological targets of cardiotonic steroids may not arise from covalent adduction. However, since drug outputs are a combination of both on- and off-target binding events, it is important to identify as many targets as possible to optimize beneficial and deleterious binding interactions, especially for pleiotropic molecules like cardenolides. Probes such as **79b** that display a toxicity profile similar to the canonical cardiotonic steroids, are thus useful for further mechanistic studies.

We finally compared effects of compounds **79a**, **92** and **97**—a set of compounds with differential oxidation of the steroid ring—against (MDA-MD-231; EC_{50} 0.111, 0.038, and 0.042 μM respectively) and an inherently-insensitive line (NIH-3T3, EC_{50}s>3 μM). We investigated how these compounds affect DNA-damage response (DDR)[36] (γ-H2AX upregulation) and apoptosis (caspase-3 activation, an early step in apoptosis) (Figure S9). We first confirmed the validity of our immunofluorescence assays using mitomycin C, which showed DDR-upregulation in MDA-MB-231 and NIH-3T3, but Caspase-3-uregulation only in NIH-3T3, Using identical assay conditions, 24 h treatment with **79a** (0.111 μM), **92** (0.038 μM) or **97** (0.042 μM) did not upregulate γ-H2AX or caspase-3 activation in NIH-3T3, consistent with the resistance of this line to cardiotonic steroids. In MDA-MB-231 cells, 24-h treatment with the same dose of these compounds upregulated both γ-H2AX and caspase-3 activation, consistent with apoptosis, possibly occurring through DDR. For all 3 compounds in MDA-MB-231 cells, there was an increase in γ-H2AX puncta, further indicating DDR as a common effect. We next compared effects in HeLa cells treated with **79a** (0.015 μM) and **92** (0.012 μM) for 24 h (Figure S10).

Figure 3. Evaluation of anticancer activity of 37 synthetic and natural cardenolides against **(A)** HEK293T and **(B)** HeLa (1 μM, 48 hr) **(C)** EC_{50} values for the 5 most potent glycosylated steroids against HEK293T, HeLa, U87, HEPG2, MDA-MB-231 and NIH-3T3. Box shows median with standard deviation; whiskers show 95% confidence intervals. (**D**) Structure of compounds **79a**, **92**, and **97.** (**E**) Toxicity studies in developing larval zebrafish at 3 μM of indicated compounds (DMSO N=38; **79a** N=35; mitomycin C N=36; brefeldin A N =38; actinomycin D N=33). **(F)** Representative data evaluating teratogenicity. Fish A: coronary edema (a bulge in cardiac tissue); B and C: normal. Fishes D and E: spinal deformities (and coronary edema).

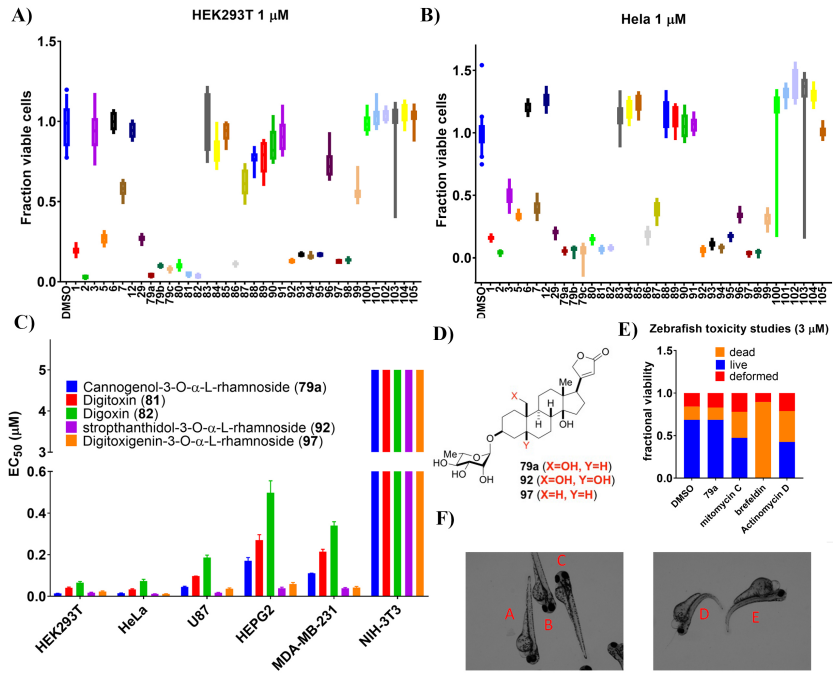

Little upregulation in caspase-3 was observed, whereas γ-H2AX was upregulated significantly with an increase in γ-H2AX foci. Staurosporine on the other hand upregulated both γ-H2AX and caspase-3. A caspase inhibitor did not affect γ-H2AX upregulation promoted by **79a** and **92**. Thus, we conclude that the mode of action for these two compounds and likely **97** follows the following order: DDR upregulation, which in turn upregulates apoptosis. Although more work needs to be done to validate the hypothesis, we propose that this mode of action (apoptosis that accompanies DDR) is common to numerous cardenolides.

3. CONCLUSION

In summary, we have developed a convergent and concise total synthesis of ouabagenin (**1**) and several other cardiotonic steroids with lower oxidation states including 11-deoxy steroids such as cannogenol (**5**) and its glycosylated analogs (**79a-b**). These syntheses enabled the subsequent SAR studies to elucidate the effect of oxygenation, stereochemistry, C3-glycosylation and C17-heterocyclic ring on the anticancer activity of the synthetic and natural cardiotonic steroids. Based on parallel evaluation of synthetic and natural steroids and their derivatives, natural products cannogenol-3-O-α–*L*-rhamnoside (**79a**) and strophanthidol-3-O-α–*L*-rhamnoside (**92**) were identified as two of the most potent analogs, demonstrating broad anticancer activity in 10-100 nM concentrations and selectivity (nontoxic at 3μM against NIH-3T3, MEF and developing fish embryos).

ASSOCIATED CONTENT

Supporting Information

Experimental procedures and ^{1}H and ^{13}C NMR spectra, are available free of charge via the Internet.

AUTHOR INFORMATION

Corresponding Authors

* nagorny@umich.edu * yimon.aye@epfl.ch * mjl253@cornell.edu

Author Contributions

All authors have given approval to the final version of the manuscript.

Funding Sources

This work was supported by NIH grant 1R01GM111476 (P.N.). We acknowledge funding from NSF grant CHE-0840456 for X-ray instrumentation. NSF CAREER (CHE-1351400), Beckman Young Investigator, NIH-New-Innovator (1DP2GM114850), Office of Naval Research (ONR) Young Investigator (N00014-17-1-2529), Novartis Foundation, and NCCR Chemical Biology, and Swiss Federal Institute of Technology Lausanne (EPFL) (to Y.A.). Cornell Imaging Center (NIH 1S10RR025502, PI: R.M. Williams) is acknowledged.

Acknowledgement

We thank Dr. Tay Rosenthal and Valentin Dorokhov for preparing compounds **91**–**96**.

REFERENCES

(1) Wasserstrom, J. A.; Aistrup, G. L. Digitalis: New Actions for an Old Drug. *Am. J. Physiol. Heart Circ. Physiol.* **2005**, *289*, H1781.

(2) (a) Ahmad, V. U.; Basha, A. *Spectroscopic Data of Steroid Glycosides: Spirostanes, Bufanolides, Cardenolides.* Chapter 3. Springer, New York, 2006, pp. 524-695; (b) Ahmad, V. U.; Basha, A. *Spectroscopic Data of Steroid Glycosides: Cardenolides and Pregnanes.* Chapter 4. Springer, New York, 2006, pp. 2089-2759.

(3) (a) Nesher, M.; Shpolansky, U.; Rosen, H.; Lichstein, D. The Digitalis-like Steroid Hormones: New Mechanisms of Action and Biological Significance. *Life Sci.* **2007**, *80*, 2093; (b) Schoner, W.; Scheiner-Bobis, G. Endogenous and Exogenous Cardiac Glycosides: Their Roles in Hypertension, Salt Metabolism, and Cell Growth. *Am. J. Phsyiol. Cell Physiol*. **2007**, *293*, C509; (c) Prassas, I.; Diamandis, E. P. Novel Therapeutic Applications of Cardiac Glycosides. *Nature Reviews* **2008**, *7*, 926; (d) Bagrov, A. Y.; Shapiro, J. I.; Fedorova, O. V. Endogenous Cardiotonic Steroids: Physiology, Pharmacology, and Novel Therapeutic Targets. *Pharm. Reviews* **2009**, *61*, 9.

(4) (a) Babula, P.; Masarik, M.; Adam, V.; Provaznik, I.; Kizek, R. From Na+/K+-ATPase and Cardiac Glycosides to Cytotoxicity and Cancer Treatment. *Anti-Cancer Agent. Med. Chem.* **2013**, *13*, 1069-1087; (b) Schneider, N. F. Z.; Cerella, C.; Simoes, C. M. O.; Diederich, M. Anticancer and Immunogenic Properties of Cardiac Glycosides. *Molecule*s **2017**, *22*, 1932.

(5) Cai, H.; Wang, H.-Y. L.; Venkatadri, R.; Fu, D.-X.; Forman, M.; Bajaj, S. O.; Li, H.; O'Doherty, G. A.; Aravboger, R. Digitoxin Analogues with Improved Anticytomegalovirus Activity. *ACS Med. Chem. Lett.* **2014**, *5*, 395.

(6) Akhtar, N.; Malik, A.; Ali, S. N.; Kazmi, S. U. Proceragenin, an Antibacterial Cardenolide from *Calotropis procera. Phytochemistry* **1992**, *31*, 2821.

(7) Jacob, P. L.; Leite, J. A.; Alves, A. K.; Rodrigues, Y. K.; Amorim, F. M.; Neris, P. L.; Oliveira, M. R.; Rodrigues-Mascarenhas, S. Immunomodulatory Activity of Ouabain in *Leishmania leishmania amazonensis*-infected *Swiss* Mice. *Prasitol. Res.* **2013**, *112*, 1313.

(8) Yoneyama, T.; Arai, M. A.; Akamine, R.; Koryudzu, K.; Tsuchiya, A.; Sadhu, S. K.; Ahmed, F.; Itoh, M.; Okamoto, R.; Ishibashi, M. Notch Inhibitors from *Calotropis gigantea* That Induce Neuronal Differentiation of Neural Stem Cells. *J. Nat. Prod.* **2017**, *80*, 2453.

(9) (a) Orellana, A. M.; Kinoshita, P. F.; Leite, J. A.; Kawamoto, M.; Scavone, C. Cardiotonic Steroids as Modulators of Neuroinflammation. *Front. Endocrinol.* **2016**, *7*, 1-10.

(10) Ferrari, P.; Ferrandi, M.; Valentini, G.; Bianchi, G. Rostafuroxin: An Ouabain Antagonist that Corrects Renal and Vascular Na^{+}-K^{+}-ATPase Alterations in Ouabain and Adducin-dependent Hypertension. *Am. J. Physiol. Regul. Integr. Comp. Physiol.* **2006**, *290*, R529.

(11) Mijatovic, T.; Kiss, R. Cardiotonic Steroids-Mediated Na+/K+-ATPase Targeting Could Circumvent Various Chemoresistance Pathways. *Planta Med.* **2013**, *79*, 189.

(12) (a) Pavlovic, D. The role of cardiotonic steroids in the pathogenesis of cardiomyopathy in chronic kidney disease. *Nephron. Clin. Pract.* **2014**, *128*, 11; (b) Calderon-Montano, J. M.; Burgos-Moron, E.; Orta, M. L.; Maldonado-Navas, D.; Garcia-Dominguez, I.; Lopez-Lazaro, M. Evaluating the cancer therapeutic potential of cardiac glycosides. *BioMed Res. Int.* **2014**, ID794930.

(13) (a) Haux, J. Digoxin is a potential anticancer agent for several types of cancer. *Med. Hypotheses* **1999**, *53*, 543; (b) McConkey, D. J.; Lin, Y.; Nutt, L. K.; Ozel, H. Z.; Newman, R. A. Cardiac glycosides stimulate Ca2+ increases and apoptosis in androgen-independent, metastatic human prostate adenocarcinoma cells. *Cancer Res.* **2000**, *60*, 3807 ; (c) Lopez-Lazaro, M.; Palma de la Pen˜a, N.; Pastor, N.; Martin-Cordero, C.; Navarro, E.; Cortes, F.; Ayuso, M. J.; Toro, M. V. Anti-tumour activity of Digitalis purpurea L. subsp heywoodii. *Planta Med.* **2003**, *69*, 701; (d) Goncalves-de-Albuquerque,

F. C.; Silva, R. A.; da Silva, I. C.; Castro-Faria-Neto, C. H.; Burth, P. Na/K Pump and Beyond: Na/K-ATPase as a Modulator of Apoptosis and Autophagy. *Molecules* **2017**, *22*, 578; (e) Simpson, C. D.; Mawji, I. A.; Anyiwe, K.; Williams, M. A.; Wang, X.; Venugopal, A. L.; Gronda, M.; Hurren, R.; Cheng, S.; Serra, S.; Beheshti, Z. R.; Datti, A.; Wrana, J. L.; Ezzat, S.; Schimmer, A. D. Inhibition of the Sodium Potassium Adenosine Triphosphatase Pump Sensitizes Cancer Cells to Anoikis and Prevents Distant Tumor Formation. *Cancer Res.* **2009**, *69*, 2739.

(14) Hiyoshi, H.; Abdelhady, S.; Segerström, L.; Sveinbjörnsson, B.; Nuriya, M.; Lundgren, T. K.; Desfrere, L.; Miyakawa, A.; Yasui, M.; Kogner, P.; Johnsen, J. I.; Andäng, M.; Uhlén, P. Quiescence and γH2AX in neuroblastoma are regulated by ouabain/Na,K-ATPase. *Br. J. Cancer.* **2012**, *106,*1807.

(15) Zhang, H.; Qian, D. Z.; Tan, Y. S.; Lee, K.; Gao, P.; Ren, Y. R.; Rey, S.; Hammers, H.; Chang, D.; Pili, R.; Dang, C. V.; Liu, J. O.; Semenza, G. L. Digoxin and other cardiac glycosides inhibit HIF-1alpha synthesis and block tumor growth. *Proc. Natl. Acad. Sci. U.S.A.* **2008**, *105*, 19579.

(16) (a) Surovtseva, Y. V.; Jairam, V.; Salem, A. F.; Sundaram, R. K.; Bindra, R. S.; Herzon, S. B. Caracterization of cardiac glycoside natural products as potent inhibitors of DNA double-strand break repair by a whole-cell double immunofluorescence assay. *J. Am. Chem. Soc.* **2016**, *138*, 3844; (b) Sun, M.; Pan, D.; Chen, Y.; Li, Y.; Gao, K.; Hu, B. Coroglaucigenin enhances the radiosensitivity of human lung cancer cells through Nrf2/ROS pathway. *Oncotarget* **2017**, *8*, 32807.

(17) Menger, L.; Vacchelli, E.; Adjemian, S.; Martins, I.; Ma, Y.; Shen, S.; Yamazaki, T.; Sukkurwala, A.Q.; Michaud, M.; Mignot, G.; Schlemmer, F.; Sulpice, E.; Locher, C.; Gidrol, X.; Ghiringhelli, F.; Modjtahedi, N.; Galluzzi, L.; André, F.; Zitvogel, L.; Kepp, O.; Kromer, G. Cardiac glycosides exert anticancer effects by inducing immunogenic cell death. *Sci Transl Med.* **2012**, *4*, 143ra99.

(18) Lopez-Lazaro, M.; Pastor, N.; Azrak, S. S.; Ayuso, M. J.; Austin, C. A.; Cortes, F. Digitoxin inhibits the growth of cancer cell lines at concentrations commonly found in cardiac patients. *J. Nat. Prod.* **2005,** *68,* 1642.

(19) Solier, S.; Pommier, Y. The nuclear γ-H2AX apoptotic ring: implications for cancers and autoimmune diseases. *Cell Mol. Life Sci.* **2014**, *71*, 2289.

(20) (a) Langenhan, J. M.; Peters, N. R.; Guzei, A. I.; Hoffmann, M.; Thorson, J. S. Enhancing the Anticancer Properties of Cardiac Glycosides by Neoglycorandomization. *Proc. Nat. Acad. Sci. U.S.A.* **2005**, *102*, 12305; (b) Iyer, A. K. V.; Zhou, M.; Azad, N.; Elbaz, H.; Wang, L.; Rogalsky, D. K.; Rojanasakul, Y.; O'Doherty, G. A.; Langenhan, J. M. A Direct Comparison of the Anticancer Activities of Digitoxin MeON-Neoglycosides and *O*-Glycosides. *ACS Med. Chem. Lett.* **2010**, *1*, 326; (c) Li, X.; Ren, Y.; Bao, Y.; Liu, J.; Zhang, X.; Zhang, Y.; Sun, X.; Yao, X.; Tang, J. Synthesis of C_3-Neoglycosides of Digoxigenin and their Anticancer Activities. *Eur. J. Med. Chem*. **2018**, *145*, 252.

(21) (a) Heasley, B. Chemical Synthesis of the Cardiotonic Steroid Glycosides and Related Natural Products. *Chem. Eur. J.* **2012**, *18*, 3092; (b) Michalak, M.; Michalak, K.; Wicha, J. The Synthesis of Cardenolide and Bufadienolide Aglycones, and Related Steroids Bearing a Heterocyclic Subunit. *Nat. Prod. Rep.* **2017**, *34*, 361; (c) Mizoguchi, H. Recent Developments in Synthetic Strategies toward Highly Oxygenated Steroids Cardenolides. *J. Synth. Org. Chem. Japan* **2017**, *75*, 253; (d) Pessoa, M. T. C.; Barbosa, L. A.; Villar, J. A. F. P. Synthesis of Cardiac Steroids and Their Role on Heart Failure and Cancer. *Stud. Nat. Prod. Chem.* **2018**, *57*, 79.

(22) For the selected recent examples highlighting the use of new approaches in the total synthesis of natural steroids and related terpenoids refer to: (a) Prevost, S.; Dupre, N.; Leutzsch, M.; Wang, Q.; Wakchaure, V.; List, B. Catalytic Asymmetric Torgov Cyclization: A Concise Total Synthesis of (+)-Estrone. *Angew. Chem. Int. Ed.* **2014**, *53*, 8770; (b) Halskov, K. S.; Donslund, B. S.; Barfusser, S.; Jorgensen, K. A. Organocatalytic Asymmetric Formation of Steroids. *Angew. Chem. Int. Ed.* **2014**, *53*, 4137; (c) Dao, H. T.; Baran, P. S. Quinone Diazides for Olefin Functionalization. *Angew. Chem. Int. Ed.* **2014**, *53*, 14382; (d) Sharpe, R. J.; Johnson, J. S. A Global and Local Desymmetrization Approach to the Synthesis of Steroidal Alkaloids: Stereocontrolled Total Synthesis of Paspaline. *J. Am. Chem. Soc.* **2015**, *137*, 4968; (e) Zhu, D.; Yu, B. Total Synthesis of Linckosides A and B, the Representative Starfish Polyhydroxysteroid Glycosides with Neuritogenic Activities. *J. Am. Chem. Soc.* **2015**, *137*, 15098; (f) Camelio, A. M.; Johnson, T. C.; Siegel, D. Total Synthesis of Celastrol, Development of a Platform to Access Celastroid Natural Products. *J. Am. Chem. Soc.* **2015**, *137*, 11864; (g) See, Y. Y.; Herrmann, A. T.; Aihara, Y.; Baran, P. S. Scalable C-H Oxidation with Copper: Synthesis of Polyoxypregnanes. *J. Am. Chem. Soc.* **2015**, *137*, 13776; (h) Logan, M. M.; Toma, T.; Thomas-Tran, R.; Du Bois, J. Asymmetric synthesis of batrachotoxin: Enantiomeric toxins show functional divergence against Na_V. *Science* **2016**, *354*, 865; (i) Xu, G.; Elkin, M.; Tantillo, D.; Newhouse, T. R.; Maimone, T. Traversing Biosynthetic Carbocation Landscapes in the Total Synthesis of Andrastin and Terretonin Meroterpenes. *Angew. Chem. Int. Ed.* **2017**, *56*, 12498; (j) Hayashi, Y.; Koshino, S.; Ojima, K.; Kwon, E. Pot Economy in the Total Synthesis of Estradiol Methyl Ether by Using an Organocatalyst. *Angew.Chem. Int. Ed.* **2017**, *56*,11812; (k) Kim, W. S.; Du, K.; Eastman, A.; Hughes, R. P.; Micalizio, G. C. Synthetic *nat*- or *ent*-Steroids in as few as Five Chemical Steps from Epichlorohydrin. *Nat. Chem*. **2017**, 10, 70; (l) Del Bel, M.; Abela, A. R.; Ng, J. D.; Guerrero, C. A. Enantioselective Chemical Syntheses of the Furanosteroids (−)-Viridin and (−)-Viridiol. *J. Am. Chem. Soc.* **2017**, *139*, 6819. (m) Liu, J.; Wu, J.; Fan, J.-H.; Yan, X.; Mei, G.; Li, C.-C. Asymmetric Total Synthesis of Cyclocitrinol. *J. Am. Chem. Soc.* **2018**, *140*, 5365; (n) Lu, Z.; Zhang, X.; Guo, Z.; Chen, Y.; Mu, T.; Li, A. Total Synthesis of Aplysiasecosterol A. *J. Am. Chem. Soc.* **2018**, *140*, 9211; (o) Goswami, S.; Harada, K.; El-Mansy, M. F.; Lingampally, R.; Carter, R. G. Enantioselective Synthesis of (-)-Halenaquinone. *Agnew. Chem. Int. Ed.* **2018**, *130,* 9255; (p) Wang, Y.; Ju, W.; Tian, H.; Tian, W.; Gui, J. Scalable Synthesis of Cyclocitrinol. *J. Am. Chem. Soc.* **2018**, *140*, 9413.

(23) (a) Stork, G.; West, F.; Lee, H. Y.; Isaacs, R. C. A.; Manabe, S. The Total Synthesis of a Natural Cardenolide: (+)-Digitoxigenin. *J. Am. Chem. Soc.* **1996**, *118*, 10660; (b) Honma, M.; Nakada, M. Enantioselective Total Synthesis of (+)-Digitoxigenin. *Tetrahedron Lett.* **2007**, *48*, 1541; (c) Jung, M. E.; Yoo, D. First Total Synthesis of Rhodexin A. *Org. Lett.* **2011**, *13*, 2698; (d) Wiesner, K.; Tsai, T. Y. R. Some Recent Progress in the Synthetic and Medicinal Chemistry of Cardioactive Steroid Glycosides. *Pure Appl. Chem.* **1986**, *58*, 799; (e) Kocovsky, P.; Stieborova, I. Synthesis of Strophanthidin. *Tetrahedron Lett.* **1989**, *30*, 4295; (f) Deng, W.; Jensen, M. S.; Overman, L. E.; Rucker, P. V.; Vionnet, J. P. A Strategy for Total Synthesis of Complex Cardenolides. *J. Org. Chem.* **1996**, *61*, 6760; (g) Overman, L. E.; Rucker, P. V. Enantioselective Synthesis of Cardenolide Precursors using an Intramolecular Heck Reaction. *Tetrahedron Lett.* **1998**, *39*, 4643; (h) Yang, Z.; Shannon, D.; Truong, V.-L.; Deslongchamps, P. Studies Directed toward Asymmetric Synthesis of Cardioactive Steroids via Anionic Polycyclization. *Org. Lett.* **2002**, *4*, 4693; (i) Jung, M. E.; Davidov, P. Efficient Synthesis of a Tricyclic BCD Analogue of Ouabain: Lewis Acid Catalyzed Diels–Alder Reactions of Sterically Hindered Systems. *Angew. Chem. Int. Ed.* **2002**, *41*, 4125; (j) Jung, M. E.; Piizzi, G. Synthetic Approach to the AB Ring System of Ouabain. *J. Org. Chem.* **2003**, *68*, 2572; (k) Michalak, K.; Morawiak, M.; Wicha, J. Synthetic Approach to the Core Structure of Oleandrin and

Related Cardiac Glycosides with Highly Functionalized Ring D. *Org. Lett.* **2016**, *18*, 6148.
(24) (a) Zhang, H.; Reddy, M. S.; Phoenix, S.; Deslongchamps, P. Total Synthesis of Ouabagenin and Ouabain. *Angew. Chem. Int. Ed.* **2008**, *47*, 1272; (b) Reddy, M. S.; Zhang, H.; Phoenix, S.; Deslongchamps, P. Total Synthesis of Ouabagenin and Ouabain. *Chem.-Asian J.* **2009**, *4*, 725.
(25) (a) Renata, H.; Zhou, Q.; Baran, P. S. Strategic Redox Relay Enables A Scalable Synthesis of Ouabagenin, A Bioactive Cardenolide. *Science* **2013**, *339*, 59; (b) Renata, H.; Zhou, Q.; Dunstl, G.; Felding, J.; Merchant, R. R.; Yeh, C.-H.; Baran, P. S. Development of a Concise Synthesis of Ouabagenin and Hydroxylated Corticosteroid Analogues. *J. Am. Chem. Soc.* **2015**, *137*, 1330.
(26) (a) Mukai, K.; Urabe, D.; Kasuya, S.; Aoki, N.; Inoue, M. A Convergent Total Synthesis of 19-Hydroxysarmentogenin. *Angew. Chem. Int. Ed.* **2013**, *52*, 5300; (b) Mukai, K.; Kasuya, S.; Nakagawa, Y.; Urabe, D.; Inoue, M. A Convergent Total Synthesis of Ouabagenin. *Chem. Sci.* **2015**, *6*, 3383.
(27) (a) Cichowicz, N.; Kaplan, W.; Khomutnik, I.; Bhattarai, B.; Sun, Z.; Nagorny, P. Concise Enantioselective Synthesis of Oxygenated Steroids via Sequential Copper(II)-Catalyzed Michael Addition/Intramolecular Aldol Cyclization Reactions. *J. Am. Chem. Soc.* **2015**, *137,* 14341; (b) Cichowicz, N.; Nagorny, P. *Strategies and Tactics in Organic Synthesis*, Volume 12, Chapter 9, **2016** (Edited by Michael Harmata), 237; (c) Lee, J.; Wang, S.; Callahan, M.; Nagorny, P. Copper(II)-Catalyzed Tandem Decarboxylative Michael/Aldol Reactions Leading to the Formation of Functionalized Cyclohexenones. *Org. Lett.* **2018**, *20,* 2067.
(28) (a) Kaplan, W.; Khatri, H. R.; Nagorny, P. Concise Enantioselective Total Synthesis of Cardiotonic Steroids 19-Hydroxysarmentogenin and Trewianin Aglycone. *J. Am. Chem. Soc.* **2016**, *138*, 7194-7198; (b) Bhattarai, B.; Nagorny, P. Enantioselective Total synthesis of cannogenol-3-*O*-α-L-rhamnoside via sequential Cu(II)-catalyzed Michael addition/intramolecular aldol cyclization reactions. *Org. Lett.*, **2018,** *20,* 154.
(29) (a) Kwan, E. E.; Scheerer, J. R.; Evans, D. A. The Stereochemical Course of Intramolecular Michael Reactions. *J. Org. Chem.* **2013**, *78*, 175; (b) Evans, D. A.; Johnson, J. S.; Olhava, E. J. Enantioselective Synthesis of Dihydropyrans. Catalysis of Hetero Diels-Alder Reactions by Bis(oxazoline) Copper(II) Complexes. *J. Am. Chem. Soc.* **2000**, *122*, 1635.
(30) (a) Keno, T.; Mil, H.; Maruoka, K. Direct Asymmetric Benzoyloxylation of Aldehydes Catalyzed by 2-Tritylpyrrolidine. *J. Am. Chem. Soc.* **2009**, *131*, 3450; (b) Vaismaa, M. J. P.; Yau, S. C.; Tomkinson, N. C. O. Organocatalytic α-Oxybenzoylation of Aldehydes. *Tetrahedron Lett.* **2009**, *50*, 3625.
(31) (a) Marigo, M.; Wabnitz, T. C.; Fielenbach, D.; Jorgensen, K. A. Enantioselective Organocatalyzed α Sulfenylation of Aldehydes. *Angew. Chem. Int. Ed.* **2005**, *44*, 794; (b) Hayashi, Y.; Gotoh, H.; Hayashi, T.; Shoji, M. Diphenylprolinol Silyl Ethers as Efficient Organocatalysts for the Asymmetric Michael Reaction of Aldehydes and Nitroalkenes. *Angew. Chem. Int. Ed.* **2005**, *44*, 4212.
(32) Ishihara, Y.; Baran, P. S. Two-Phase Terpene Total Synthesis: Historical Perspective and Application to the Taxol® Problem. *Synlett* **2010**, *12*, 1733.
(33) Engman, L.; Stern, D. Thiol/Diselenide Exchange for the Generation of Benzeneselenolate Ion. Catalytic Reductive Ring-Opening of -Epoxy Ketones. *J. Org. Chem.* **1994,** *59***,** 5179.
(34) Jing, Y.; Xu, C-G.; Ding, K.; Lin, J.-R.; Jin, R.-H.; Tian, W.-S. Protecting group effect on the 1,2-dehydrogenation of 19-hydroxysteroids: a highly efficient protocol for the synthesis of estrogens. *Tetrahedron Lett.* **2010**, *51,* 3242.
(35) Diao,T.; Stahl, S.-S. Synthesis of Cyclic Enones via Direct Palladium-Catalyzed Aerobic Dehydrogenation of Ketones. *J. Am. Chem. Soc*. **2011**, *133*, 14566.
(36) McIntyre, D.-D.; German, M.-W; Vogel, H.-J. Conformational Analysis and Complete Assignment of the Proton and Carbon NMR Spectra of Ouabain and Ouabagenin. *Can. J. Chem*. **1990**, *68*, 1263-1270.
(37) (a) Jiang, M.-M. Dai, Y.; Gao, H.; Zhang, X.; Wang, G.-H.; He, J.-Y.; Hu, Q.-Y.; Zheng, J.-Z.; Zhang, X.-K.; Yao, X.-S. Cardenolides from *Antiaris toxicaria* as Potent Selective Nur77 Modulators. *Chem. Pharm. Bull.* **2008**, *56*, 1005; (b) Shi, L.-S.; Kuo, S.-C.; Sun, H.-D.; Morris-Natschke, S. L.; Lee, K.-H.; Wu, T.-S. Cytotoxic Cardiac Glycosides and Coumarins from *Antiaris toxicaria. Bioorg. Med. Chem.* **2014**, *22*, 1889; (c) Tian, D.-M.; Cheng, H.-Y.; Shen, W.-Z.; Tang, J.-S.; Yao, X.-S. Cardiac Glycosides from the Seeds of *Thevetia peruviana. J. Nat. Prod.* **2016**, *79*, 38.
(38) Banuls, L. M. Y.; Urban, E.; Gelbcke, M.; Dufrasne, F.; Kopp, B.; Kiss, R.; Zehl, M. Structure–Activity Relationship Analysis of Bufadienolide-Induced in Vitro Growth Inhibitory Effects on Mouse and Human Cancer Cells. *J. Nat. Prod.* **2013**, *76*, 1078.
(39) (a) Calderon-Montano, J. M.; Burgos-Moron, E.; Lopez-Lazaro, M. Comment on 'Quiescence and γH2AX in neuroblastoma are regulated by Ouabain/Na,K-ATPase': ouabain and cancer. *Br. J. Cancer.* **2013**,*108*, 2189; (b) Gupta, R. S.; Chopra, A.; Stetsko, D. K.; Cellular basis for the species differences in sensitivity to cardiac glycosides (digitalis). *J. Cell Physiol.* **1986**, *127*, 197.
(40) Pathak, S.; Multani, A. S.; Narayan, S.; Kumar, V.; Newman, R. A. AntiverzelTM, an extract of Nerium oleander, induces cell death in human, but not murine cancer cells. *Anticancer Drugs* **2000**, *11*, 455.
(41) Goessling W.; Allen R. S.; Guan, X.; Jin, P.; Uchida, N.; Dovey, M.; Harris, J. M.; Metzger, M. E.; Bonifacino, A. C.; Stroncek, D.; Stegner, J.; Armant, M.; Schlaeger, T.; Tisdale, J. F.; Zon, L. I.; Donahue, R. E.; North, T. E. Prostaglandin E2 enhances engraftment of human cord blood stem cells and shows long-term safety in preclinical non-human primate transplant models. *Cell Stem Cell* **2011**, *8*, 445.
(42) (a) Arai, Y.; Pulvers, J. N.; Haffner, C.; Schilling, B.; Nusslein, I.; Calegari, F.; Huttner, W. B. Neural stem and progenitor cells shorten S-phase on commitment to neuron production. *Nature Commun*. **2011**, *154*, 1; (b) Yuet, K. P.; Doma, M. K.; Ngo, J. T.; Sweredoski, M. J.; Graham, R. L. J.; Moradian, A.; Hess, S.; Schuman, E. M.; Sternberg, P. W.; Tirrell, D. A. Cell-specific proteomic analysis in *Caenorhabditis elegans*. *Proc*. *Natl*. *Acad*. *Sci*., *U*. *S*. *A*. **2015**, *112*, 2705.

Unified Synthetic Approach to Cardenolides

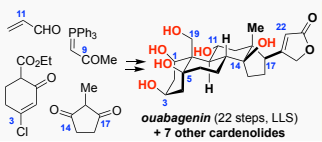

Anticancer Activity Evaluation

> 37 compounds are evaluated against 3 cell lines
> Highly active (10-100 nm IC_{50}) compounds identified
> Non-toxic at 3 μM (NIH-3T3, MEF, fish embryos)
> Structure Activity Relationship (SAR) analysis
> Likely modification of intracellular target
> Possible covalent binding to intracellular targets
> DNA-damage induction and subsequent apoptosis